Materials Physics and Mechanics 47 (2021) 399-407 Received: April 27, 2021

CRYSTALLOGRAPHIC TEXTURE OF INDUSTRIAL AUTOMOTIVE STEELS AND EFFECT OF TERTIARY CEMENTITE DISSOLUTION ON ITS DEVELOPMENT

A.A. Vasilyev[1*], N.Y. Zolotorevsky[1], D.F. Sokolov[2], S.A. Philippov[1]

[1]Peter the Great St. Petersburg Polytechnic University, Polytekhnicheskaya, 29, 195251, St. Petersburg, Russia

[2]PJSC Severstal, Mira, 30, 162608, Cherepovets, Russia

*e-mail: vasilyev_aa@mail.ru

Abstract. X-ray investigation of crystallographic texture and its correlation with r_m value (Lankford coefficient) was performed on a representative set of industrial automotive steels of different grades. Though the majority of steels had the structure of polygonal ferrite with small fractions of pearlite in the hot rolled condition, steels with a more complex structure were also included in the study. For this set of steels, a linear dependency has been shown to hold between r_m value and the logarithm of the ratio of volumes having orientations of {111} and {100} planes parallel to the sheet plane. It is proposed that the observed reduction of r_m value with increasing carbon content in steel is caused by the dissolution of tertiary cementite during recrystallization annealing.

Keywords: automotive steels, annealing, recrystallization, texture, tertiary cementite

1. Introduction

Control of crystallographic texture is important for various applications, where it intends to obtain beneficial anisotropy of physical and mechanical properties by developing favorable preferred crystal lattice orientations [1,2]. For example, the texture is a critical characteristic in the production of silicon steels for magnetic applications, since α-iron crystals have a significant anisotropy in magnetization [3]. Furthermore, it is significant for steels used under low temperatures, e.g. in Arctic condition, because cleavage cracks develop preferentially along {100} planes [4]. Another effect, which is just the subject of the present investigation, relates to the development of low-carbon steels for application in the automotive industry. The problem appears owing to the fact that anisotropy of crystal plasticity influences the deep drawability of sheet metal, in particular, the orientation of the {111} planes parallel to the sheet plane turns out to be favorable, while {100} – unfavorable [1,5]. It is possible through control of steel composition and processing route to optimize the relation between the fractions of grains having above orientations [1].

The common measure of deep drawability is the plastic strain ratio (r value or Lankford coefficient), which is determined in tensile tests and is the ratio of strains in the width and thickness directions of the sheet specimen [6]. Since r values vary depending on the test direction, an average r_m value is commonly defined on the base of the strain ratio measurements in directions at 0°, 45° and 90° to the rolling direction of the sheet: $r_m = ¼ (r_0 + 2r_{45} + r_{90})$. Although the deep drawability may depend on different material characteristics, the significance of the texture was thoroughly established. In particular, a

http://dx.doi.org/10.18149/MPM.4732021_1

linear dependency was shown to exist between r_m value and the logarithm of the ratio of the volumes having {111} and {100} orientations [1].

Despite the importance of the texture, its impact on the deep drawability of automotive steels was studied insufficiently. An only rather narrow range of compositions, including pure iron and some purely ferritic steels, were examined previously in connection with 'drawability *vs.* texture' dependency [1,6]. Furthermore, the final temperature of recrystallization annealing conducted under industrial conditions may exceed the critical temperature, above which phase transformation to austenite occurs. Nevertheless, it was not studied to date if an additional transformation circle could influence the texture. The presented study aimed at enhancing our knowledge of this matter. An investigation of crystallographic texture, as well as its correlations with r_m value, was carried out for a set of industrial automotive steels of different grades. In addition, the mechanism, by which a dissolution of cementite formed at ferrite grain boundaries before cold rolling can influence the texture development during recrystallization annealing is proposed.

2. Framework of texture analysis

X-ray diffractometry is employed commonly in texture determination. Based on measured intensity distributions for X-ray reflection from various crystallographic planes, the orientation distribution function (ODF) is then calculated. When using ODF, an orientation is represented by a point with coordinates (φ_1, Φ, φ_2) in the space of Euler angles. Owing to crystal symmetry, only a small part of this orientation space is sufficient for the description of the texture. Moreover, in many cases, only a section of the part of orientation space is used. In the case of the steel sheet, it is the section φ_2=45°, within which all orientations important for our research are located (Fig. 1). During the processing of steel, crystallographic texture experiences several transformations: it appears first under hot rolling and then changes under cooling due to phase transformation, under cold rolling, and subsequent annealing. The latest stage of texture evolution is of interest for us in the present study.

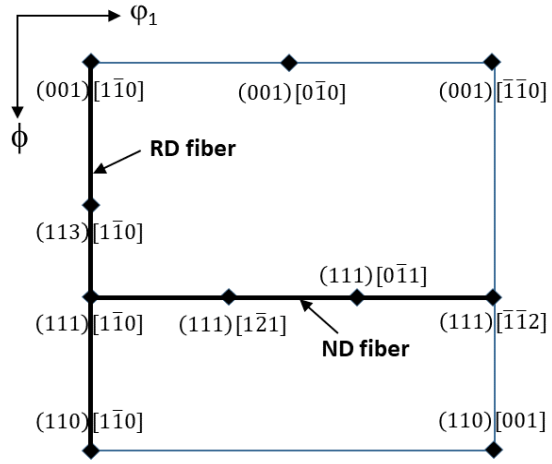

Fig. 1. φ_2 = 45° section of Euler space showing the steel texture components

Principal preferential orientations, which present in metal after cold rolling, are included in so-called 'fibers' shown in Fig. 1 by thick lines [2,7]. The orientations having the {111} planes parallel to the rolling plane (sheet plane) constitute ND-fiber, while the orientations having <110> axis parallel to the rolling direction – RD-fiber. In the course of recrystallization under annealing of the cold-rolled sheet the fraction of orientations

comprising the RD-fiber decreases, while orientations comprising the ND-fiber increase. Naturally, the recrystallization texture depends on the texture of cold-rolled sheet. In addition, it has been shown in earlier researches that the recrystallization texture is affected by the chemical composition of steel [1,8].

3. Experimental

The chemical compositions of steels examined in the present study are shown in Table 1. The 2000 mill at PJSC Severstal was used for hot rolling. After cold rolling, the strip is heat-treated in the line for continuous annealing and galvanizing. Table 2 shows some technological parameters and results of steel characterization.

Table 1. Chemical compositions of the investigated steels (mass.%)

Steel	C	Mn	Si	Cr	Nb	Ti
H220YD	0.004	0.50	0.10	–	–	0.064
DX54D	0.005	0.10	–	–	–	0.061
CR210B2	0.005	0.54	–	–	0.016	0.016
HX220BD	0.005	0.63	–	–	0.015	0.021
HX260YD	0.006	0.72	0.10	–	–	0.066
08Ю*)	0.05	0.16	–	–	–	–
HX300LAD	0.06	0.32	–	–	0.023	0.014
08ПС*)	0.07	1.18	–	–	–	–
CR420LA	0.09	0.83	–	–	0.061	–
DP600	0.09	1.65	0.20	0.44	–	–
DP780	0.14	1.84	–	0.34	0.026	–
S320GD	0.18	0.45	0.23	–	–	–

*) Russian grades

Table 2. Parameters of industrial treatment (cold rolling reduction ε_{cr}, annealing temperature T_a), critical temperatures A_{p1} and A_{p3} calculated using Thermo-Calc under para-equilibrium condition, r_m values determined, and structure types after hot rolling. PF − polygonal ferrite, P – pearlite, B – bainite

Steel	ε_{cr}, %	T_a, °C	A_{p1}, °C	A_{p3}, °C	r_m	Structure type
HX220YD	0.67	774	–	899	2.18	PF
DX54D	0.57; 0.79	830	–	923	2.37	
CR210B2	0.68	818	–	901	2.03	
HX220BD	0.72	801	–	906	1.60	
HX260YD	0.65	753	–	890	2.18	
08Ю*)	0.79	736	723	882	1.45	PF + ~4%P
HX300LAD	0.68	814	724	875	1.25	PF + ~5%P
08ПС*)	0.72	790	726	875	1.41	PF + ~6%P
CR420LA	0.54	749	709	834	0.75	PF + ~20%(P+B)
DP600	0.66	794	690	797	0.90	PF + ~50%(P+B)
DP780	0.61	787	685	770	0.74	PF + ~20%(P+B)
S320GD	0.58	742	715	838	1.20	PF + ~20%P

The strain ratios r_0, r_{45} , and r_{90} needed for the calculation of r_m were determined using the standard industrial method by averaging measurements conducted on three specimens. Before cold rolling, the majority of steels had the structure of polygonal ferrite with small fractions of pearlite. At the same time, steels having a more complex structure in the hot

rolled condition (Table 2) were also included in the study. One can see from Table 2 that annealing temperature in most cases exceeds A_{p1}, and hence one can expect additional phase transformation during annealing and subsequent cooling. For steels having a purely ferritic structure or a small percentage of pearlite, a negligible or very limited austenitization could be expected. However, this is not the case for the last four types of steel. In particular, almost 100% austenitization occurs in DP600 steel giving a considerable fraction of hard martensite constituent in the final structure.

X-ray diffraction analysis was carried out on the specimens cut from the steel sheets after annealing. Additionally, DX54D steel has been examined after cold rolling to reductions of 57% and 79%. Specimen preparation for X-ray analysis included mechanical and chemical polishing to remove the surface layer with a thickness of about 200 μm. Primary pole figures were measured using a specialized texture diffractometer developed in the Polytechnic University and supplied with an original system for automated texture registration. On the base of three incomplete pole figures (polar angle ψ was varied from 0° to 70°) {220}, {200} and {211} determined experimentally, the ODFs were reconstructed and the ratio of {111} and {100} contributions, referred to as (111)/(100) ratio below, was calculated for every specimen with the help of MTEX software [9].

4. Results and discussion

In order to demonstrate the character of texture development under cold rolling and subsequent annealing, the ODF obtained in steel DX54D after reductions of 57% and 79% are presented in Fig. 2.

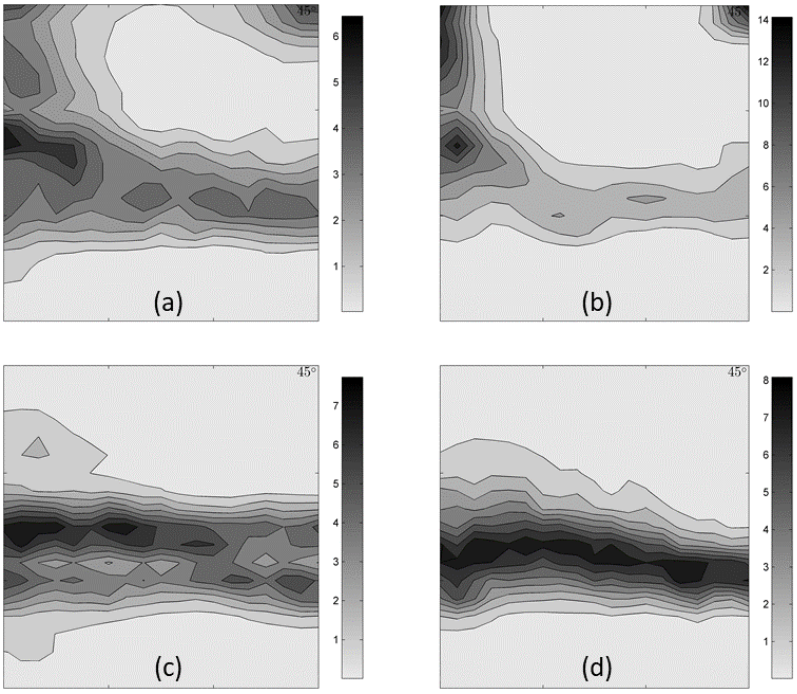

Fig. 2. Textures developed under cold rolling (a,b) and annealing (c,d) in steel DX54D after rolling reductions of 57% (a,c) and 79% (b,d). φ_2 = 45° sections of Euler space are shown

One can see in Figs. 2a and b that preferential orientations developed after cold rolling are concentrated within ND and RD fibers and additionally the texture component {001}<110> appears. The increase of cold reduction results in a considerable increase in

texture sharpening, which mainly occurs owing to the RD fiber enhancement. Further evolution of texture under annealing also proceeds in accordance with literature data [2], namely, a fraction of ND fiber increases, whereas the component {001}<110> and a part of orientations, which took place in the RD fiber, disappear (Figs. 2c and d). As a result, the relative fraction of the volume with the orientation of {111} planes parallel to the sheet plane increases considerably. It should be emphasized that, despite the fact that cold rolling texture strongly sharpens with increasing reduction, the recrystallization textures shown in Figs. 2c and d differ insignificantly.

The textures, qualitatively similar to those shown in Figs. 2b and d, was observed after annealing for all other steels. Nevertheless, variations of the (111)/(100) ratio are remarkable. Results of its determination are shown in Fig. 3 in relation to r_m value. One can see that a good linear correlation between the decimal logarithm of this ratio and r_m value occurs for this set of steels, which agrees with the correlation observed earlier for low-carbon ferritic steels [9]. Naturally, a considerable scattering of the data takes place. This is due to both the inaccuracy of texture measurement and the presence of other factors, besides the texture, which influence the deep drawability [1].

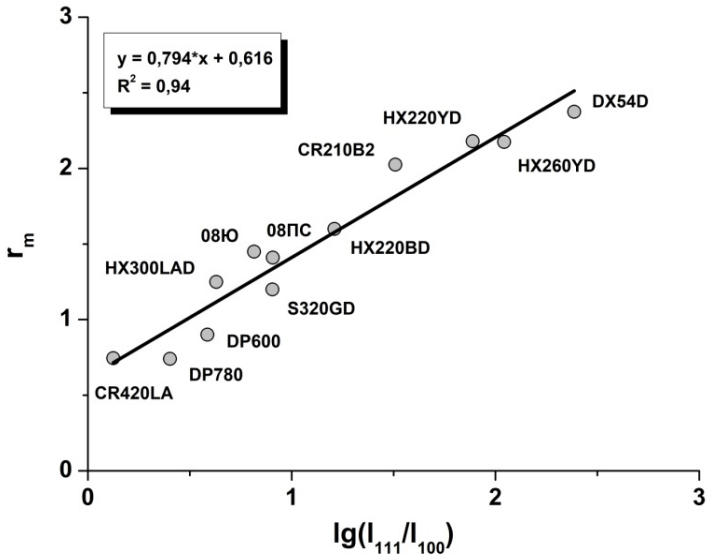

Fig. 3. Dependence of r_m value on the decimal logarithm of the ratio of the volumes having orientations {111} and {100}

A quantitative model has been earlier developed in order to predict r_m values for industrial sheets of automotive steels manufactured by PJSC Severstal [11]. It enables the calculation of r_m as a function of the chemical composition, the microstructure parameters defined by computer modeling, and the cold rolling reduction. An equilibrium carbon concentration in ferrite, w_{C_fer}, at the end of austenite transformation proceeding under cooling, is one of the important parameters of this model. Its value is computed with the help of STAN 2000 program, in which a physically-based quantitative model of austenite decomposition is implemented [12]. Figure 4a shows the dependency of r_m value on w_{C_fer} for the steels examined in the present study and additionally for the steels of the same grades used when developing the model described in Ref. [11]. The dependency of (111)/(100) ratio on w_{C_fer} plotted to base on the correlation between this ratio and r_m value (Fig. 3) is presented in Fig. 4b. It shows a good correlation, which is especially marked for steels with relatively high

carbon content. It is worth noting that the data for DP steels were not used for the calculation of the correlation curve.

A question arises, why the phase transformations occurring in the course of final annealing do not disturb the above correlation. Explanation seemingly relates to the phenomenon of "texture inheritance" observed when parent and daughter phases are connected by certain orientation relationships [2]. In particular, it was shown recently that the crystallographic texture of the state obtained after austenitization reproduces the texture formed previously [10]. Hence, the effect of texture on deep drawability is controlled by the orientation distribution formed on the stage of recrystallization, whether subsequent austenitization takes place or not.

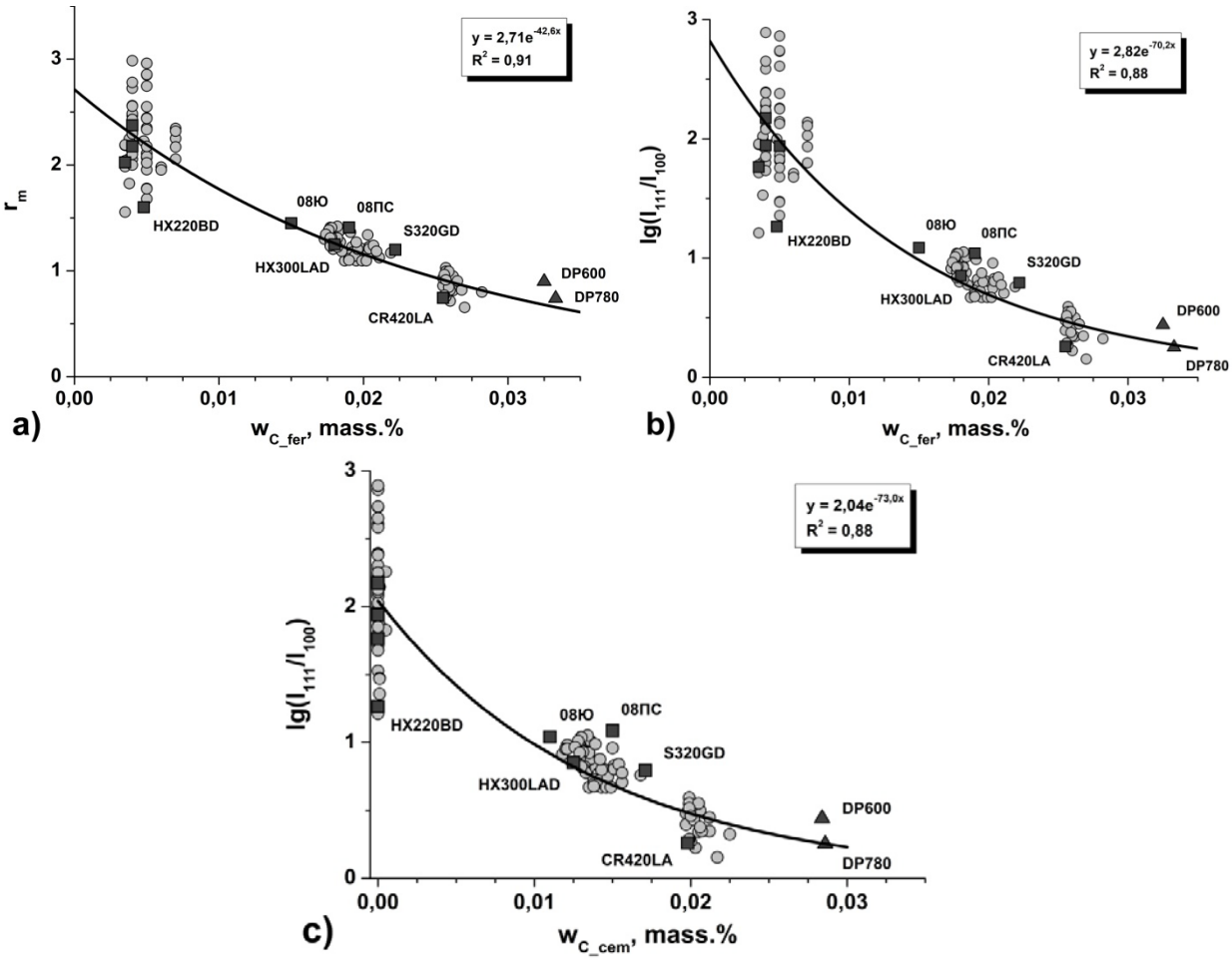

Fig. 4. Correlation of r_m value and I_{111}/I_{100} ratio with carbon-related parameters: r_m value as function of w_{C_fer} (a); I_{111}/I_{100} ratio as function of w_{C_fer} (b) and w_{C_cem} (c). Black squares relate to the steels examined in the present study and grey circles – to the steels of the same grades used when developing the model described in Ref. [11]

The impact of carbon, which appears in solid solution due to dissolution of cementite under heating, on (111)/(100) ratio was noted previously [8,11]. The physical mechanism of this effect remains, however, unclear, and thus it is interesting to discuss it in what follows. Anticipating the discussion, the dependency of (111)/(100) on the mass fraction of tertiary cementite, w_{C_cem}, calculated with STAN 2000 program is presented in Fig. 4c.

It is well known that the nucleation of new grains during recrystallization is orientation-dependent [13,14]. In the case of low-carbon steels, it was established that the nucleation of {111} grains proceeds considerably faster than {100} grains [13]. Furthermore, the amount of potential nucleation sites of certain orientation is limited resulting in their exhaustion during recrystallization, so that the nucleation rate as a function of heating time may be qualitatively represented with bell-shaped curves as shown in Fig. 5 [13-16].

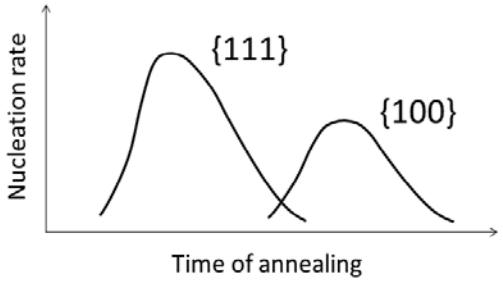

Fig. 5. Schematic representation of the nucleation rate for grains of different orientation

In addition to the above general principles of "orientational nucleation", some structural aspects of the grain nucleation should be mentioned before turning to the discussion of the carbon effect. In a cold-rolled steel, regions with orientations of type {111} <uvw> (RP-fiber in Fig. 1) are characterized by relatively high Taylor factors and therefore high level of stored energy as well as by sharp and relatively high angle subboundaries. Alternatively, the regions with orientations near {001}<110> (starting point of the RD-fiber) are characterized by the lowest Taylor factor and therefore relatively low stored energy as well as by diffuse boundaries with only minor misorientations [7]. Two mechanisms of nucleation occur in steels after moderate cold reductions [14]. The first is the strain-induced boundary migration (SIBM) which is the dominant mechanism for low rolling reductions. The second is the abnormal growth of deformation-induced subgrains possessing sufficiently mobile high angle boundaries with their surroundings. With the increasing reduction, the second mechanism becomes predominant for nucleation of {111} grains due to the appearance of high angle boundaries in the deformation structure. At the same time, only the mechanism of SIMB remains available for {100} nuclei by way of their growth into the adjacent grain of type {110} and {111} having high stored energy.

Let us now return to the carbon effect. In the IF-steels (HX220YD, DX54D, CR210B2, HX220BD, HX260YD) with $w_{C\_fer} < 0.007$ mass.% the carbon concentration in solid solution remains almost unchanged during hot-rolled strip cooling to room temperature after austenite transformation and during subsequent heating after cold rolling. In steels with higher carbon content, in contrast, excessive carbon precipitates at the ferrite grain boundaries as tertiary cementite under cooling. Subsequently, during annealing, this cementite dissolves, and, correspondingly, local carbon concentration at the boundaries of ferrite grains and in adjacent areas increases.

Previously it was suggested that mobility of grain boundaries increases with increasing carbon concentration as a result of lowering of effective activation energy of grain boundary self-diffusion [17]. This, in its turn, may lead to an acceleration of grain boundary bulging. Such a peculiarity of carbon effect is hardly of great importance for nucleation of {111} grains which may evolve from subgrains located both near grains boundaries and in the distance from them. However, it is essential for {100} grains, because the critical event for the nucleation by SIMB is a local migration (bulging) of the grain boundary. Moreover, since, on the one hand, local carbon concentration gradually increases during heating and, on the other, (100) grains nucleate later than (111) ones (Fig. 5), the accelerating effect of carbon

would be stronger for (100) nuclei even if only SIBM mechanism operates for nuclei of both orientations. Therefore, one can suggest that the dissolution of tertiary cementite is the cause of the reduced I_{111}/I_{100} ratio in steels with increased carbon content.

5. Conclusions

The existence of linear dependency between the texture characteristics $\lg(I_{111}/I_{100})$ and r_m value was obtained for a representative set of low-carbon steels with various microstructures. It was suggested that local increase of carbon concentration at grain boundaries occurring due to dissolution of tertiary cementite increases the fraction of {100} grains in the recrystallized condition. Therefore, the reduction of r_m value with increasing carbon content is explained by the effect of cementite dissolution.

Acknowledgements. *No external funding was received for this study.*

References

[1] Hutchinson WB. Development and control of annealing textures in low-carbon steels. *International Metals Reviews*. 1984;29(1): 25-42.
[2] Jonas JJ. Transformation textures associated with steel processing. In: Haldar A, Suwas S, Bhattacharjee D. (Eds.) *Microstructure and Texture in Steels and Other Materials*. 1st Edition. 2009. p.3-17.
[3] Matsuo M. Texture control in the production of grain oriented silicon steels. *Iron and Steel Institute of Japan International*. 1989;29: 809-827.
[4] Terasaki H, Shintome Y, Komizo Y, Ohata M, Moriguchi K, Tomio Y. Effect of close-packed plane boundaries in a Bain zone on the crack path in simulated coarse grained HAZ of bainitic steel. *Metallurgical and Materials Transactions* A. 2015;46A: 2035-2039.
[5] Hutchinson WB. Practical aspects of texture control in low carbon steel. *Materials Science Forum*. 1994;157-162: 1917-1928.
[6] Hutchinson WB. Critical assessment 16: Anisotropy in metals. *Materials Science and Technology*. 2015;31: 1393-1401.
[7] Hutchinson WB. Deformation microstructures and textures in steels. *Philosophical Transactions of the Royal Society*. 1999;357: 1471-1485.
[8] Hutchinson WB. Effects of cementite dissolution and carbon diffusion upon the recrystallization behaviour of low carbon steel. *Materials Science Forum*. 2002;408-412: 1167-1172.
[9] Bachmann F, Hielscher R, Schaeben H. Texture analysis with MTEX – Free and open source software toolbox. *Solid State Phenomena*. 2010;160: 63-68.
[10] Lobanov ML, Pyshmintsev IY, Urtsev VN, Danilov SV, Urtsev NV, Redikultsev AA. Texture inheritance in the ferrito-martensite structure of low-alloy steel after thermomechanical controlled processing. *Physics of Metals and Metallography*. 2019;120(12): 1180-1186.
[11] Vasilyev AA, Sokolov DF, Sokolov SF, Glukhov PA, Kolbasnikov NG, Mitrofanov AV. Model for predicting the Lankford coefficient of industrial sheet of automotive steels. *Steel in Translation*. 2018;48(2): 109-115.
[12] Ogoltcov A, Sokolov D, Sokolov S, Vasilyev A. STAN 2000: Computer model for simulation of steel hot rolling on mill 2000 of Severstal. *Materials Science Forum*. 2016;854: 183-189.
[13] Haessner F. (Ed.) *Recrystallization of metallic materials*. Second edition. Rieder Verlag GmbH, Stuttgart; 1978.
[14] Humphreys FJ, Hatherly M. *Recrystallization and related annealing phenomena*. Second edition. Oxford, UK: Elsevier; 2004.

[15] Dillamore IL, Smith CJE, Watson TW. Oriented nucleation in the formation of annealing textures in iron. *Metal Science Journal*. 1967;1: 49-54.
[16] Hutchinson WB, Artymowicz D. Mechanisms and modelling of microstructure/texture evolution in Interstitial-Free Steel Sheets. *Iron and Steel Institute of Japan International*. 2001;41(6): 533-541.
[17] Vasilyev AA, Kolbasnikov NG, Rudskoy AI, Sokolov DF, Sokolov SF. Kinetics of structure formation in the heating of cold-rolled automotive steel sheet. *Steel in Translation*. 2017;47: 830-838.